Waferscale nanophotonic circuits made from diamond-on-insulator substrates

P. Rath,[1] N. Gruhler,[1] S. Khasminskaya,[1] C. Nebel,[2]
C. Wild,[2,3] and W. H. P. Pernice[1,*]

[1]*Institute of Nanotechnology, Karlsruhe Institute of Technology, 76344 Eggenstein-Leopoldshafen, Germany*
[2]*Fraunhofer Institute for Applied Solid State Physics, Tullastr. 72, 79108 Freiburg, Germany*
[3]*Diamond Materials, Tullastr. 72, 79108 Freiburg, Germany*
[*]*wolfram.pernice@kit.edu*

Abstract: Wide bandgap dielectrics are attractive materials for the fabrication of photonic devices because they allow broadband optical operation and do not suffer from free-carrier absorption. Here we show that polycrystalline diamond thin films deposited by chemical vapor deposition provide a promising platform for the realization of large scale integrated photonic circuits. We present a full suite of photonic components required for the investigation of on-chip devices, including input grating couplers, millimeter long nanophotonic waveguides and microcavities. In microring resonators we measure loaded optical quality factors up to 11,000. Corresponding propagation loss of 5dB/mm is also confirmed by measuring transmission through long waveguides.

References

1. R. Kirchain and L. Kimerling, "A roadmap for nanophotonics," Nat. Photonics **1**(6), 303–305 (2007).
2. B. Jalali and S. Fathpour, "Silicon photonics," J. Lightwave Technol. **24**(12), 4600–4615 (2006).
3. R. Soref, "The past, present and future of silicon photonics," IEEE J. Sel. Top. Quantum Electron. **12**(6), 1678–1687 (2006).
4. W. Bludau, A. Onton, and W. Heinke, "Temperature dependence of the band gap of silicon," J. Appl. Phys. **45**(4), 1846 (1974).
5. A. Gondarenko, J. S. Levy, and M. Lipson, "High confinement micron-scale silicon nitride high Q ring resonator," Opt. Express **17**(14), 11366–11370 (2009).
6. E. Shah Hosseini, S. Yegnanarayanan, A. H. Atabaki, M. Soltani, and A. Adibi, "High quality planar silicon nitride microdisk resonators for integrated photonics in the visible wavelength range," Opt. Express **17**(17), 14543–14551 (2009).
7. K. Fong, W. Pernice, M. Li, and H. Tang, "High Q optomechanical resonators in silicon nitride nanophotonic circuits," Appl. Phys. Lett. **97**(7), 073112 (2010).
8. M.-C. Tien, J. F. Bauters, M. J. R. Heck, D. T. Spencer, D. J. Blumenthal, and J. E. Bowers, "Ultra-high quality factor planar Si3N4 ring resonators on Si substrates," Opt. Express **19**(14), 13551–13556 (2011).
9. Y. Okawachi, K. Saha, J. S. Levy, Y. H. Wen, M. Lipson, and A. L. Gaeta, "Octave-spanning frequency comb generation in a silicon nitride chip," Opt. Lett. **36**(17), 3398–3400 (2011).
10. I. Aharonovich, A. Greentree, and S. Prawer, "Diamond photonics," Nat. Photonics **5**(7), 397–405 (2011).
11. S. Castelletto, J. Harrison, L. Marseglia, A. Stanley-Clarke, B. Gibson, B. Fairchild, J. Hadden, Y.-L. Ho, M. Hiscocks, K. Ganesan, S. Huntington, F. Ladouceur, A. Greentree, S. Prawer, J. O'Brien, and J. Rarity, "Diamond-based structures to collect and guide light," New J. Phys. **13**(2), 025020 (2011).
12. B. J. Hausmann, B. Shields, Q. Quan, P. Maletinsky, M. McCutcheon, J. T. Choy, T. M. Babinec, A. Kubanek, A. Yacoby, M. D. Lukin, and M. Loncar, "Integrated diamond networks for quantum nanophotonics," Nano Lett. **12**(3), 1578–1582 (2012).
13. J. Riedrich-Möller, L. Kipfstuhl, C. Hepp, E. Neu, C. Pauly, F. Mücklich, A. Baur, M. Wandt, S. Wolff, M. Fischer, S. Gsell, M. Schreck, and C. Becher, "One- and two-dimensional photonic crystal microcavities in single crystal diamond," Nat. Nanotechnol. **7**(1), 69–74 (2011).
14. A. Faraon, C. Santori, Z. Huang, V. M. Acosta, and R. G. Beausoleil, "Coupling of nitrogen-vacancy centers to photonic crystal cavities in monocrystalline diamond," Phys. Rev. Lett. **109**(3), 033604 (2012).
15. M. Füner, C. Wild, and P. Koidl, "Novel microwave plasma reactor for diamond synthesis," Appl. Phys. Lett. **72**(10), 1149 (1998).

16. D. Taillaert, W. Bogaerts, P. Bienstman, T. F. Krauss, P. Van Daele, I. Moerman, S. Verstuyft, K. De Mesel, and R. Baets, "An out-of-plane grating coupler for efficient butt-coupling between compact planar waveguides and single-mode fibers," IEEE J. Quantum Electron. **38**(7), 949–955 (2002).
17. A. Faraon, P. Barclay, C. Santori, K. Fu, and R. Beausoleil, "Resonant enhancement of the zero-phonon emission from a colour centre in a diamond cavity," Nat. Photonics **5**(5), 301–305 (2011).
18. C. F. Wang, Y.-S. Choi, J. C. Lee, E. L. Hu, J. Yang, and J. E. Butler, "Observation of whispering gallery modes in nanocrystalline diamond microdisks," Appl. Phys. Lett. **90**(8), 081110 (2007).
19. X. Checoury, D. Neel, P. Boucaud, C. Gesset, H. Girard, S. Saada, and P. Bergonzo, "Nanocrystalline diamond photonics platform with high quality factor photonic crystal cavities," Appl. Phys. Lett. **101**(17), 171115 (2012).

1. Introduction

Nanophotonic devices are receiving continued attraction because of the possibility to integrate large-scale, monolithic photonic circuits with electronic circuits [1]. By employing silicon as photonic base material established fabrication routines originally developed for the realization of electronic integrated circuits can be directly used to create high-quality photonic structures. In particular silicon-on-insulator (SOI) wafers have enabled densely integrated photonic circuits with excellent performance in a range of applications [2,3]. However, silicon waveguides are restricted to operation wavelengths above 1100 nm as a result of the relatively small bandgap (1.1 eV [4]). For wider band applications covering visible wavelengths, photonic devices have to be realized in different material systems that are compatible with silicon fabrication processes. Within the group of wide bandgap semiconductors, silicon nitride (Si_3N_4) has attracted particular interest for the realization of CMOS compatible nanophotonic devices [5–9].

Recently diamond has emerged as a novel material for realizing optical components due to attractive material properties, such as high chemical and mechanical stability, high thermal conductivity and biocompatibility [10,11]. Because of an even larger bandgap compared to silicon nitride of 5.5 eV, diamond is transparent from ultra-violet wavelengths up into the infrared regime. To date, a variety of optical components has been fabricated from single crystalline diamond films, which are transferred onto suitable substrates using bonding procedures [12,13]. After thinning of the remaining diamond layer to a thickness of a few hundred nanometers (as required for the realization of nanophotonic waveguides) the analogous substrate to SOI, namely diamond-on-insulator (DOI), is obtained [14]. This approach however inherently limits the size of the optical circuits that can be realized because of the restricted dimensions of diamond single crystals and also requires sophisticated substrate processing techniques that reduce the device yield.

Here we present a new platform for integrated optics based on polycrystalline diamond thin films. By employing a chemical vapor deposition approach waferscale substrates with a diameter up to six inch can be readily fabricated, allowing for the realization of large area photonic devices. Under optimized growth conditions microcrystalline diamond thin films with good optical transparency are obtained without the need for a post-growth polishing step. Using a combination of electron beam lithography and dry etching we demonstrate essential components for on-chip optical circuits, including waveguides, input grating coupler and optical cavities. Fabricated microring resonators are coupled to feeding waveguides allowing us to achieve critical coupling with high extinction ratio as well as to determine the waveguide propagation loss. Both with ring resonators and long waveguides we measure propagation loss of 5 dB/mm, limited by the as-grown surface roughness. Best quality factors of 11,000 in weakly coupled devices illustrate the potential of DOI as a convenient template for optical circuits and sensing applications.

2. Substrate preparation and device fabrication

Diamond provides a relatively high refractive index of 2.4, allowing for concentrating light into nanophotonic waveguides. To enable waveguiding, the diamond layer from which the waveguides are prepared needs to be sufficiently thin and surrounded by a material with lower refractive index, acting as a cladding layer. To fabricate the devices used in the current study, we employ diamond-on-insulator substrates with a layer structure that resembles SOI wafers.

Silicon carrier wafers are thermally oxidized to a thickness of 2.0 μm to provide an optical buffer layer with low refractive index. Subsequently diamond thin films are deposited onto the oxide using chemical vapor deposition (CVD). First a diamond nano-particle seed layer is deposited onto the SiO_2 film by ultrasonification for 30 minutes in a water based suspension of ultra-dispersed (0.1 wt %) nano-diamond particles of typically 5-10 nm diameter. Then the samples are rinsed with de-ionized water and methanol. After dry blowing, the wafer is transferred into an ellipsoidal 915 MHz microwave plasma reactor [15] where diamond films of with a target thickness of 600 nm are grown at 1.8 kW microwave power. Feeding gas containing 2% methane diluted in 98% hydrogen is used at a pressure of 80mbar and a substrate temperature of 850 °C. Substrate rotation is applied to avoid angular non-uniformities arising from the gas flow. Growth rates are typically in the range of 1-2 μm/h. The diamond film thickness is controlled by timed growth combined with in situ interferometric measurement to allow for precise thickness monitoring. After growth the samples are cleaned in concentrated HNO_3:H_2SO_4 to remove surface contaminations. The above procedure leads to uniform diamond films with a grain size on the order of 100 nm without significant film defects. Without surface polishing the as-grown surface roughness is on the order of 15 nm rms, as determined from atomic force microscope measurements.

Optical circuits are then patterned using electron beam lithography on a JEOL 5300 50kV system. We employ Fox15 negative tone resist with a thickness of 500 nm in order to provide sufficient protection for subsequent dry etching. A thick layer of e-beam resist also guarantees that the diamond surface is completely covered so that no diamond peaks are exposed to the later plasma. The developed circuits are etched into the diamond layer using reactive ion etching in O_2/Ar_2 chemistry at a pressure of 20 μbar and a power of 200 W (CCP) leading to an etch rate of about 25nm/min on an Oxford 80 system. Fabricated devices are shown in Fig. 1(a).
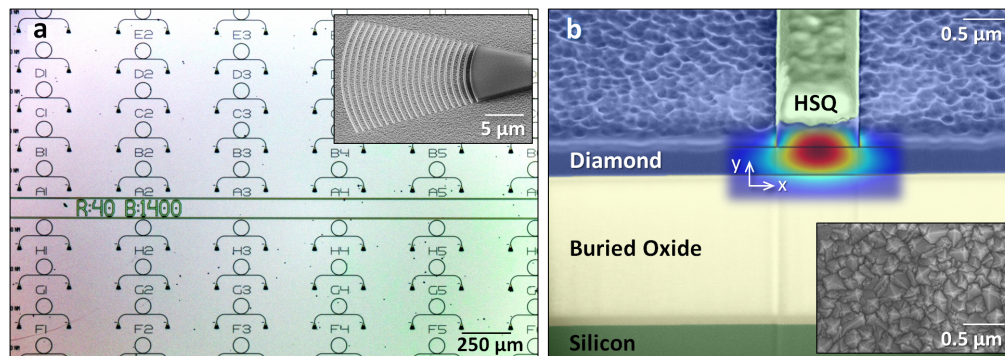

Fig. 1. a) Optical micrograph of a fabricated chip with photonic circuits consisting of focusing grating couplers, partially etched waveguides and microring resonators with 40 μm radius. Inset: SEM picture of a focusing grating coupler b) False-color SEM image of a FIB cross-section through a diamond nanophotonic ridge waveguide. Inset: Diamond surface before etching, showing the surface roughness present. Overlay: Simulated distribution of the electric field in x-direction (TE-like mode) of the ridge DOI waveguide.

The waveguides are partially etched ridge waveguides with a step height of 300 nm. The etch depth is controlled by timed etching and confirmed by white-light interferometry. From a cross-sectional image through a finished waveguide we find that near-vertical sidewalls are obtained, as also apparent in the false-color SEM image in Fig. 1(b). The cross-section is obtained using focused ion beam (FIB) milling, which leads to the artificial lines in Fig. 1(b) at the edges of the waveguide. The surface roughness at the top of the waveguide remains under the HSQ, the inset of Fig. 1(b) shows a SEM micrograph of the unetched diamond surface. On top of the waveguide the remaining HSQ e-beam resist is clearly visible, illustrating the high etching selectivity even against the RIE plasma.

3. Waveguide-coupled microring resonators

Using the fabrication procedure described above we design photonic circuitry to characterize the waveguiding properties of CVD diamond structures. In order to couple light into on-chip waveguides we employ compact focusing grating couplers [16]. With optimized filling factor and grating period a coupling loss of −5.0 dB at the central coupling wavelength is achieved, in par with silicon photonic grating devices. Because we use partially etched gratings, the effective refractive index mismatch of the grating to the fiber is smaller compared to fully etched silicon grating couplers, leading to a large 3 dB coupling bandwidth of 50nm. The central coupling wavelength can be adjusted by varying the period of the grating. In our case we select a central wavelength of 1550 nm within the telecoms C-band.

We then characterize the optical properties of the microrings by measuring transmission through the circuits. Light from a tunable laser source (New Focus Venturi 6600) is coupled into the chip through an optical fiber array at an input grating coupler and collected at a second grating coupler at the output. Many different circuits on fabricated chips can be measured conveniently by aligning the fiber array to pairs of grating couplers with a computer-controlled three-axis piezo-stage. The transmitted optical signal is collected with a low-noise photodetector (New Focus 2011). On-chip photonic cavities can then be characterized via coupling to a feeding waveguide enclosed between grating couplers as depicted in Fig. 1(a). Here we use microring resonators with radii from 40 to 70 μm, as shown for exemplary devices in the optical image in Fig. 1(a). The waveguide width of the feeding waveguide is kept at 1 μm to ensure single-mode guiding. The microrings are separated from the feeding waveguide by a narrow coupling gap, which is varied across several devices in order to vary the coupling condition into the ring. Typical transmission spectra for 40 μm rings are shown in Fig. 2(a) for near-critically coupled devices.
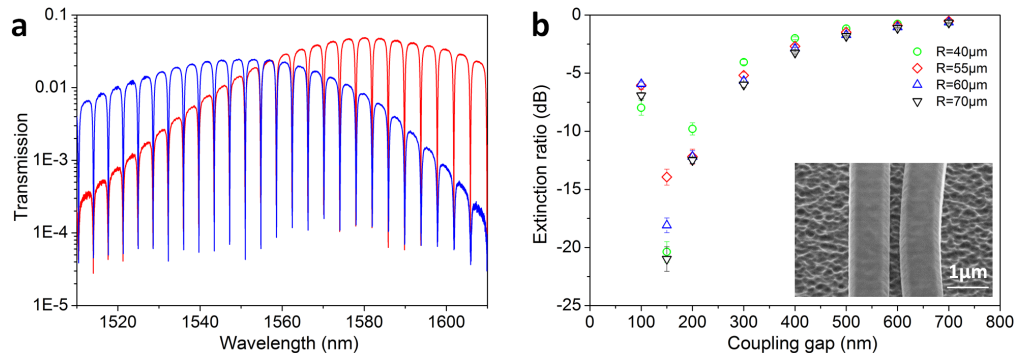

Fig. 2. a) Typical transmission spectra for a near-critically coupled ring resonator devices with 40 μm radius showing resonances with a free-spectral range of 3.79 nm, enveloped by the profile of the grating coupler. The spectra are shown for two devices with the same coupling gap, but different central wavelength of the grating coupler. b) Measured extinction ratios depending on the coupling gap, near-critically coupled show extinction ratios exceeding 20 dB. Inset: SEM picture of the gap region between ring resonator and feeding waveguide.

Several resonances are visible in the transmission spectrum, which is enveloped by the coupling profile of the grating coupler. From the separation between neighboring fringes we extract a free-spectral range of 3.79 nm and thus a corresponding group index of 2.52. The group index obtained from the measurement data is in good agreement with the value of 2.53 of the TE-like mode simulated with finite-element software (COMSOL Multiphysics). The resulting mode profile is shown as an overlay in Fig. 1(b). By changing the coupling gap between the ring resonator and the waveguide the coupling condition can be chosen. When the gap is set to 150 nm, the rings are near-critically coupled. In this case we obtain high extinction ratios up to 30 dB. When the separation to the feeding waveguide is increased, the rings are operated in the weakly coupled regime, where the microring is not heavily loaded. By increasing the gap more and more the ring is decoupled further from the feeding

waveguide, meaning that it allows us to study its intrinsic properties to first order approximation. In this case the extinction ratio is strongly reduced as shown in Fig. 2(b) and almost vanishes for coupling gaps larger than 700 nm. Similarly, for heavily loaded rings at small coupling gaps, the extinction ratio also decreases from the maximum value at critical coupling. For increasing ring radii a reduced bending loss is expected which manifests in a larger extinction ratio at the same coupling gap and an improving quality factor (not shown) compared to smaller microrings. For radii larger than 55 µm no further increase in the extinction ratio at larger coupling gaps was found, suggesting that the bending loss becomes a minor loss channel.

By fitting the resonance dip with a Lorentzian function we can extract the optical quality factor. We study whether an increasing ring width leads to a reduced propagation loss. For this purpose the ring width is varied from 1.0 to 1.6 µm. The measured values in dependence of coupling gap for rings operated in the various coupling regimes are shown in Fig. 3(a). Each data point corresponds to the average of 5 to 10 resonances of one ring resonator; the error bar shows the standard deviation.
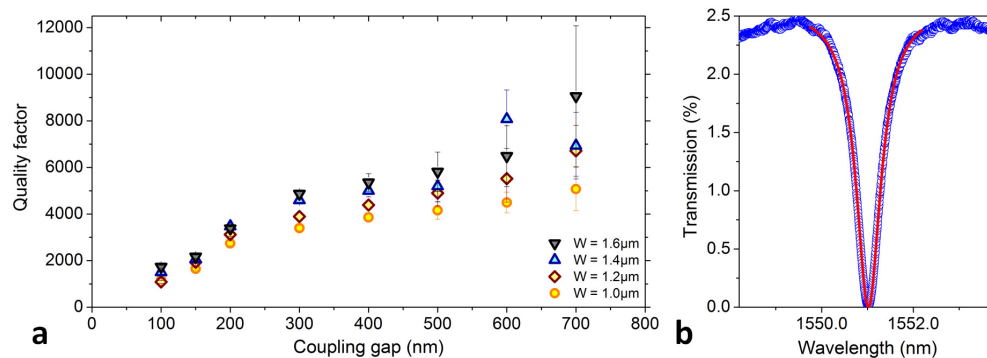

Fig. 3. a) The measured dependence of the optical quality factor of 55 µm rings on the coupling gapsize and ring width. Best Q factors of 11,000 are obtained for weakly coupled devices. b) The Lorentzian fit (red) to a resonance of a near-critically coupled ring cavity, showing 28dB extinction ratio and a quality factor of 2400.

It can be seen that the quality factor improves with increasing waveguide width due to the fact that the guided mode has less overlap with the surface roughness. For critically coupled rings of 55 µm radius we measure typical linewidths on the order of 500 pm. In the weakly coupled regime we obtain higher Q values, with an average quality factor of 9,060 for a width of 1.6 µm. Several devices show best values above 11,000, in par with results reported in ref [17]. for single crystalline diamond at 650 nm and two orders of magnitude better than values reported for polycrystalline diamond microdisks [18].

From the optical quality factor the propagation loss of the fabricated waveguides can be extracted using the relation $\alpha = 10\log_{10} e \cdot 2\pi n_g / Q_{int}\lambda$ (where Q_{int} is the intrinsic quality factor, λ the wavelength and n_g is the group index). Plugging in the measured Q-values yields a propagation loss of 4.7 dB/mm for 1.6 µm wide, half etched diamond ridge waveguides. Because we are using as-grown diamond thin films the propagation loss is most likely limited by scattering due to the intrinsic surface roughness. This value could be improved in future work by applying surface polishing procedures.

4. Measurement of the propagation loss with long waveguides

To confirm the induced propagation loss from the previous section we perform independent measurements of transmission through long diamond ridge waveguides of 1 µm width. In order to preserve chip real estate the waveguides are arranged in a meander pattern as shown for a set of devices in Fig. 4 (a). The length of the waveguide is increased between rows of devices and the transmission through each is measured using the procedure described above.

In order to account for the coupling loss occurring at the input grating coupler we use a balanced measurement approach with an additional reference port.
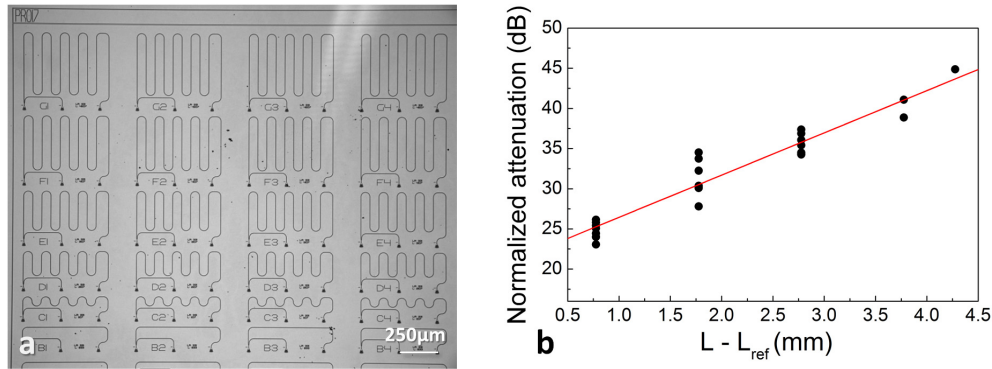

Fig. 4. a) An optical microscope image of a section of a fabricated chip, showing several meandering waveguides with lengths up to 4600 µm. Neighboring columns contain identical devices with varying grating coupler period, to enable a statistical estimation of the error bar. b) Measurement results for the normalized attenuation in the test waveguides, showing a propagation loss of 5.3 ± 0.3 dB/mm.

Light coupled into the circuit is split at the input grating coupler using a 50/50 Y-splitter. Then the transmitted signal is recorded at the two output ports simultaneously with two independent photodetectors. The transmission through the long arm of the device is then normalized to the reference port, taking into account the propagation distance through the reference arm. Results for devices with different lengths are shown in Fig. 4(b). We vary the device length in the long arm from 770 µm to 4.6 mm, which leads to increasing propagation loss. The normalized attenuation in units of dB is plotted over the waveguide length. By fitting the data with a line we can obtain the propagation loss as 5.3 ± 0.3 dB/mm, in good agreement with the loss obtained from the measurement of the ring resonators. The measured loss is a factor of five smaller than reported recently for polycrystalline diamond, even without surface polishing [19]. The results thus illustrate that waveguiding over millimeter distances is possible with our diamond substrates.

5. Conclusions

Contrary to previous beliefs we have shown here that polycrystalline CVD diamond is a suitable material system for the realization of on-chip photonic circuits. By employing a plasma-enhanced growth procedure DOI substrates can be prepared with waferscale dimensions, suitable for mass fabrication of photonic circuits. Even without surface polishing we obtain a significantly reduced propagation loss and ring resonators with quality factors in par with previous demonstrations in single-crystalline diamond thin films. However, our approach does not involve sophisticated wafer pre-processing techniques, leading to simple manufacture with high yield.